THE JOURNAL OF PHYSICAL CHEMISTRY A
A JOURNAL OF THE AMERICAN CHEMICAL SOCIETY

pubs.acs.org/JPCA

Article

Reimagining the Wave Function in Density Functional Theory: Exploring Strongly Correlated States in Pancake-Bonded Radical Dimers

Luis Rizo and Benjamin G. Janesko*

Cite This: J. Phys. Chem. A 2023, 127, 3684−3691

Read Online

ACCESS | Metrics & More | Article Recommendations

ABSTRACT: Pancake bonding between π-conjugated radicals challenges conventional electronic structure approximations, due to the presence of both dispersion (van der Waals) interactions and "strong" electron correlation. Here we use a reimagined wave function-in-density functional theory (DFT) approach to model pancake bonds. Our generalized self-interaction correction extends DFT's reference system of noninteracting electrons, by introducing electron−electron interactions within an active space. We show that a small variation on our previous derivation recovers a DFT-corrected complete active space method proposed by Pijeau and Hohenstein. Comparison of the two approaches shows that the latter provides reasonable dissociation curves for single bonds and pancake bonds, including excited states inaccessible to conventional linear response time-dependent DFT. The results motivate broader adoption of wavefunction-in-DFT approaches for modeling pancake bonds.

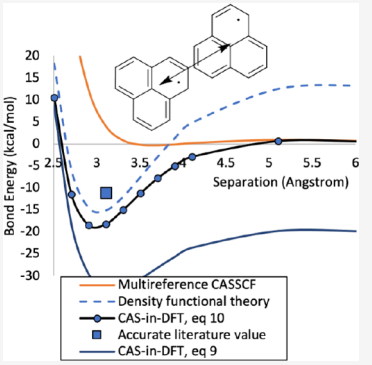

INTRODUCTION

Strong electron correlation in large systems remains an outstanding challenge in electronic structure theory. Strong correlation can occur in stretched covalent bonds,[1] twisted double bonds,[2] diradicaloids,[3] molecular magnets,[1] mixed-valence oxides,[4] large π-conjugated systems,[5−7] and any other system whose wave function is poorly described by a single molecular orbital (MO) configuration (single Slater determinant wave function). Kohn−Sham density functional theory (DFT) adds density-based corrections to a single MO configuration, an approach that is practical for large systems but often unreliable for strong correlation.[8] Multireference correlated wave function approaches provide accurate and systematically improvable treatments of strong correlation, but their high computational cost and non-black-box character (see refs 9, 10) can limit routine application to large systems.

For decades, theorists have explored wavefunction-in-DFT approaches intended to combine these methods' strengths without inheriting too many of their weaknesses.[11−23] Our Adiabatic Projection correction[24,25] employs a flexible generalization of the range-separated adiabatic connection[22] (used in, for example, long-range density matrix renormalization group[26] or long-range random phase approximations[19]), combined with a density functional correction inspired by the Perdew−Zunger self-interaction correction.[27] In the present work, we use the projected interaction correction to explore pancake bonds.

PANCAKE BONDING

Pancake bonding provides a "hard but not too hard" example of strong correlation in large systems. Pancake bonds involve dimerization of π-conjugated radicals via multicenter two-electron bonds. This highly directional interaction produces a parallel π-stacked geometry and a shorter-than-van-der-Waals monomer separation.[28] In the solid state, pancake bonding can contribute large bandwidths and high conductivities to organic functional materials.[29] In molecular complexes, pancake bonding contributes an open-shell diradicaloid character[30] and a fluxional bonding providing stimulus-responsive color and magnetism,[31] and has been hypothesized to contribute to asphaltene aggregation in petroleum crude oil.[32]

Computationally, pancake bonds' strong correlation is largely localized to the radical electrons. Extant multireference simulations of the phenalenyl dimer require only two active orbitals.[33−35] Standard DFT approaches can provide reasonably accurate predictions for pancake bond ground states near equilibrium.[36,37] However, DFT's performance for full potential energy surfaces is less well characterized. In the present work, we will show that our generalized self-interaction

Received: December 8, 2022
Revised: February 21, 2023
Published: April 13, 2023

https://doi.org/10.1021/acs.jpca.2c08616
J. Phys. Chem. A 2023, 127, 3684−3691

correction[25] provides a derivation of a wave function-in-DFT *ansatz* proposed by Pijeau and Hohenstein.[21] This approach proves to be well-suited for modeling pancake bonds.

THEORY

Generalized Self-Interaction Correction. Our approach is based on the generalized range-separated adiabatic connection.[11,13,15,17−19,22,38,39] For completeness, we briefly review that method here. We consider a calculation on an N-electron system. In standard Kohn−Sham DFT, we introduce a reference system of N noninteracting electrons, whose wavefunction is treated exactly by a single Slater determinant. The Hohenberg−Kohn theorems ensure that the real system's ground-state energy and density can be obtained from an exact wave function calculation on the noninteracting reference system, corrected by a density functional for the Hartree-exchange-correlation (HXC) energy.[19] The Runge-Gross theorem ensures that excited states are also available from the reference system.[40]

In the generalized range-separated adiabatic connection, one separates the electron−electron interaction operator $\hat{V}_{ee}$ into short-range and long-range pieces. Part of the interaction, typically the long-range part, is reintroduced into the reference system. The Hohenberg−Kohn theorems ensure that the real system's ground-state energy and density can be obtained from an exact wave function calculation on the long-range-interacting reference system, corrected by a density functional for the remaining short-range HXC energy.[19] The exact short-range HXC functional may be obtained from an adiabatic connection integration. This approach is formally rigorous, systematically improvable, and ensures that no part of the electron−electron interaction is "double-counted".[41]

Adiabatic Projection. Our Adiabatic Projection approach extends this generalized range-separated adiabatic connection. Rather than separating $\hat{V}_{ee}$ into short-range and long-range pieces, we project $\hat{V}_{ee}$ onto an active space. More specifically, we consider an N-electron system whose strong correlation can be effectively modeled by a complete active space (CAS) wave function, including N_e active electrons in N_a active orbitals $\{|\psi_p^a\rangle\}$ and $N_c = (N - N_a)/2$ doubly occupied core orbitals $\{|\psi_i^c\rangle\}$. (For neutral phenalenyl dimer, we use $N = 174$, $N_e = 2$, $N_a = 2$.) Indices p, q, r, s denote active orbitals, indices i, j, k, l denote core orbitals. We define a two-electron projection operator onto the active space

$$\hat{P}_a(m, n) = \sum_{p,q=n_c+1}^{n_c+n_o} \psi_p^a(m)\psi_q^{a*}(n)\psi_p^a(m)\psi_q^{a*}(n) \tag{1}$$

and a projected electron−electron interaction operator

$$\hat{V}_{ee}^P = \sum_{m,n=1}^{N} \hat{P}_a(m, n)\frac{1}{r_{mn}}\hat{P}_a(m, n) \tag{2}$$

(The notation $\hat{P}_a(m, n)$ means that the two-electron operator acts on electrons m and n.) We introduce the projected operator into the reference system. Because the reference system only includes electron−electron interactions within the active space, a CAS wavefunction can provide the exact ground-state of the projected-interacting reference system. The Hohenberg−Kohn theorems ensure that the real system's ground-state energy and density can be obtained from an exact wave function calculation on the projected-interacting reference system, corrected by a density functional for the remaining projected HXC energy. The exact projected HXC functional may be formally defined by an adiabatic connection. The ground-state energy of the real system E_0 is the ground-state energy of the projected-interacting reference system E_{ref}^P, corrected by this projected HXC density functional:

$$E_0 = E_{\text{ref}}^P + E_{\text{HXC}}^P[\rho_P] \tag{3}$$

More explicitly, let γ and Γ denote the one-electron and two-electron reduced density matrices obtained from the reference system's CAS wave function. (Note that $\gamma_{ij} = 2\delta_{ij}$ for the core orbitals.) Let $\mathbf{t}$ and $\mathbf{v}$ denote the kinetic energy and external potential operators. The ground-state energy of the projected-interacting reference system is

$$E_{\text{ref}}^P = \sum_i \gamma_{ii}(t_{ii} + v_{ii}) + \sum_{pq} \gamma_{pq}(t_{pq} + v_{pq}) + \sum_{pqrs} \Gamma_{pqrs}\langle pq||rs\rangle \tag{4}$$

(Note that the projected-interacting reference system does not include electron interactions outside of the active space, just as the long-range-interacting reference system introduced in the range-separated adiabatic connection does not include short-range electron−electron interactions, and the Kohn−Sham reference system does not include any electron−electron interactions.) The Hartree component of the projected HXC energy $E_{\text{HXC}}^P[\rho]$ combines core−core and core−active Hartree energies

$$E_{\text{Hartree}}^P = \frac{1}{2}\sum_{ij} \gamma_{ii}\gamma_{jj}\langle ij|ij\rangle + \frac{1}{2}\sum_{ipq} \gamma_{ii}\gamma_{pq}\langle ip|iq\rangle \tag{5}$$

The projected XC energy also combines core−core and core−active terms. For example, we may define the projected Hartree−Fock-like "exact" exchange as

$$E_{\text{HFX}}^P = E_{\text{HFX}}^{\text{CC}} + E_{\text{HFX}}^{\text{CA}} \tag{6}$$

$$E_{\text{HFX}}^{\text{CC}} = -\frac{1}{2}\sum_{ij} \gamma_{ii}\gamma_{jj}\langle ij|ji\rangle \tag{7}$$

$$E_{\text{HFX}}^{\text{CA}} = -\frac{1}{2}\sum_{ipq} \gamma_{ii}\gamma_{pq}\langle ip|qi\rangle \tag{8}$$

With this definition, the expectation value of the real system's Hamiltonian, evaluated using the reference system's CAS wave function, becomes $E_0(\text{CAS}) = E_{\text{ref}}^P + E_{\text{Hartree}}^P + E_{\text{HFX}}^{\text{CC}} + E_{\text{HFX}}^{\text{CA}}$.

To proceed, we must choose an approximation for the projected XC functional in eq 3. A trivial choice is to model the projected XC functional as exact nonlocal exchange and no correlation, eqs 6−8. With this choice, the ground-state energy of the real system is modeled as $E_0(\text{CAS})$. This is analogous to standard generalized Kohn−Sham DFT, where one can choose to model the entire XC functional as exact exchange. With this choice, the ground-state energy of the real system is modeled as the Hartree−Fock total energy.

In our previous work, we chose to model the projected XC functional using a standard density functional approximation for the entire core−core and core−active XC energy. We use "DFA" to denote a density functional approximation for exchange-correlation, and denote the corresponding core−core

https://doi.org/10.1021/acs.jpca.2c08616
J. Phys. Chem. A 2023, 127, 3684−3691

and core−active energies as E_{DFA}^{CC} and E_{DFA}^{CA}. We use $E_{DFA}[\gamma]$ to specify a DFA evaluated using the electron density (and potentially the density gradient, noninteracting kinetic energy density, density Laplacian, and nonlocal exact exchange) obtained from one-particle density matrix γ. With this choice, the ground-state energy of the real system is modeled as

$$\begin{aligned} E_0 &= E_{ref}^{P} + E_{Hartree}^{P} + E_{DFA}^{CC+CA} \\ &= E_0(CAS) - (E_{HFX}^{CC} + E_{HFX}^{CA}) + E_{DFA}[\gamma] - E_{DFA}[\gamma_a] \end{aligned} \tag{9}$$

The Hartree−Fock-like core−core and core−active exchange interactions present in E_0(CAS) are subtracted off in eq 9, and replaced with the DFA, ensuring that there is no double-counting of exchange. The active-space one-particle density matrix is defined as $\gamma_a(\mathbf{r}, \mathbf{r}') = \sum_{pq} \psi_p(\mathbf{r})\psi_q^*(\mathbf{r}')\gamma_{pq}$ In our previous work, we motivated this choice as a generalization of the Perdew−Zunger self-interaction correction.[27] We showed that replacing the single active space projection $\hat{P}_a(m, n)$ in eq 1 with a sum of projections onto individual localized MOs $\hat{P}_i(m, n) = \psi_i(m)\psi_i(n)\psi_i(m)\psi_i(n)$ ensures that the reference system includes only electron self-interaction, and that the reference system's ground-state wave function is a single Slater determinant as in standard DFT. Combining this projection with the choice of projected XC functional outlined above precisely recovers the Perdew−Zunger self-interaction correction.[42] A similar "wavefunction-in-DFT" approximation was proposed previously by Malcolm and McDouall, without derivation and with a restriction to exact exchange.[14]

Here, we show that a slightly different choice for the projected XC functional recovers the density functional correction to complete active space configuration interaction energies proposed by Pijeau and Hohenstein.[21] One may choose to model the core−active piece of the projected XC functional using exact exchange, and model only the core−core piece with a density functional $E_{DFA}[\gamma_c]$. The core-space one-particle density matrix γ_c is defined as $\gamma_c(\mathbf{r}, \mathbf{r}') = \sum_i \psi_i(\mathbf{r})\psi_i^*(\mathbf{r})\gamma_{ii}$, where as noted above $\gamma_{ij} = 2\delta_{ij}$ for the core orbitals. With this choice, the ground-state energy of the real system is modeled as

$$\begin{aligned} E_0 &= E_{ref}^{P} + E_{Hartree}^{P} + E_{HFX}^{CA} + E_{DFA}^{CC} \\ &= E_0(CAS) - E_{HFX}^{CC} + E_{DFA}[\gamma_c] \end{aligned} \tag{10}$$

Both eqs 9 and 10 recover standard DFT when there are no active electrons ($N_a = 0$) and recover full CI where all electrons and orbitals are active.

Pijeau and co-workers have identified interesting properties of eq 10. Calculations with this approach correctly dissociate single bonds and can improve on the Hartree−Fock description of the part of the system outside of the active space.[21] These authors have used eq 10 to model excited states, combining excited-state CASCI with a standard ground-state DFA.[21,43] Such calculations recover CASCI vertical excitation energies computed with a given set of nuclear coordinates. While the authors framed this approach as an alternative to semiempirical CI methods, the present work suggests instead that eq 9 and eq 10 are well-defined approximations to the exact projected XC functional in eq 3. The remainder of this work presents numerical results comparing eqs 9 and 10, and a discussion of their merits for modeling large polyradical aromatics.

COMPUTATIONAL DETAILS

Most calculations use the PySCF electronic structure package.[44] PySCF implementation of eq 9 and eq 10 is freely available online at github.org/bjanesko/. Calculations with eqs 9 and 10 use orbitals obtained from CASSCF calculations. Fully self-consistent evaluation of the orbitals will be explored in future work. Ref 45 discusses the role of orbital choice in active-space calculations. Unless noted otherwise, all DFT calculations use spin-symmetry-restricted Hartree−Fock orbitals. Ground-state dissociation energies of all dimers are computed relative to twice the monomer ground-state energy. For example, CAS(2e,2o)SCF calculations on the ground-state dissociation energy of neutral chlorine and phenalenyl dimers are compared to CAS(1e,1o) (equivalent to restricted open-shell Hartree−Fock) calculations on open-shell chlorine atom and phenalenyl molecule, respectively. The right-hand panel of Figure 4 shows that calculations with eq 10 correctly recover a dimer dissociation energy of zero at large separations. Calculations on Cl_2 use the def2-TZVP basis set.[46] Calculations on phenalenyl dimer use the 6-31G(d) basis set following refs 34, 35, and frozen monomer geometries taken from ref 34.

Reference values for the Cl_2 ground state are obtained from new N-electron valence perturbation theory (NEVPT2) simulations, based on a CAS(2e,2o)SCF reference. Reference values for the equilibrium bond length and bond energy of neutral phenalenyl dimer in the lowest-energy singlet and triplet states are taken from multireference coupled cluster[47] MR-AQCC(2,2)/6-31G(d) calculations reported in ref 34. Reference values for the positively charged dimer are from MR-AQCC calculations reported in ref 35.

Figure 4 reports results from several standard DFAs: the local spin-density approximation LDA,[48] the Becke-Lee−Yang−Parr (BLYP)[49,50] and PBE generalized gradient approximations (GGAs), the Tao-Perdew-Staroverov-Scuseria (TPSS),[51] strongly constrained and appropriately normed (SCAN),[52] and M06L[53] and MN15L[54] meta-GGAs, the global hybrids B3LYP,[55] O3LYP,[56] M05, M05-2X, and M06.[57] Calculations in Figure 6 use orbitals from a state-averaged CAS(2e,2o)SCF calculation on the three lowest-energy states (two singlets and one triplet). As in previous work,[21] calculations with eq 10 combine a ground-state DFA with orbitals and density matrices from the CASSCF excited states.

RESULTS

Chlorine Dimer. We begin by comparing eqs 9 and 10 for a model system, the $X^1\Sigma_g^+$ singlet ground-state potential energy surface of chlorine dimer Cl_2. Calculations with eq 9 and eq 10 use a minimal CAS(2e,2o) active space of the Cl−Cl bond's bonding and antibonding orbitals and the Perdew−Burke−Ernzerhof (PBE) DFA.[58] Figure 1 shows the computed PES. The NEVPT2 reference calculations in Figure 1 give a dissociation energy D_e = 56.9 kcal/mol close to the 2.49 eV (57.4 kcal/mol) obtained in earlier multireference simulations.[59] CAS(2e,2o)SCF underbinds. While both eq 9 and eq 10 give accurate results near equilibrium, eq 9 gives a severely overbound dissociation limit, 33 kcal/mol below the energy of two Cl atoms. Equation 10 recovers the correct dissociation limit, as seen for other single bonds.[21]

https://doi.org/10.1021/acs.jpca.2c08616
J. Phys. Chem. A 2023, 127, 3684−3691

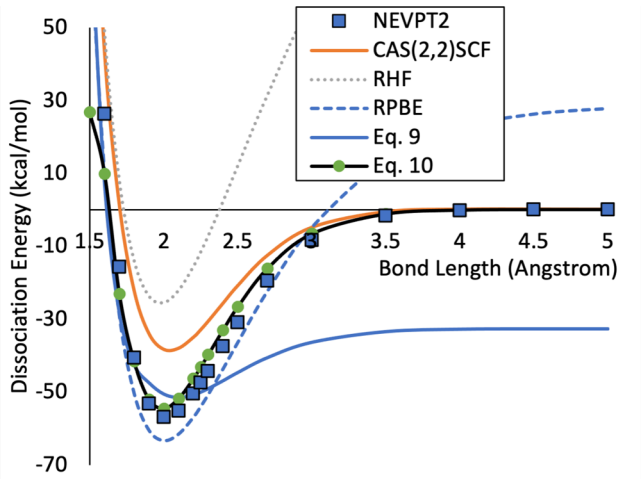

Figure 1. Ground-state singlet potential energy surface of chlorine dimer Cl_2, energy relative to two ground-state Cl* atoms.

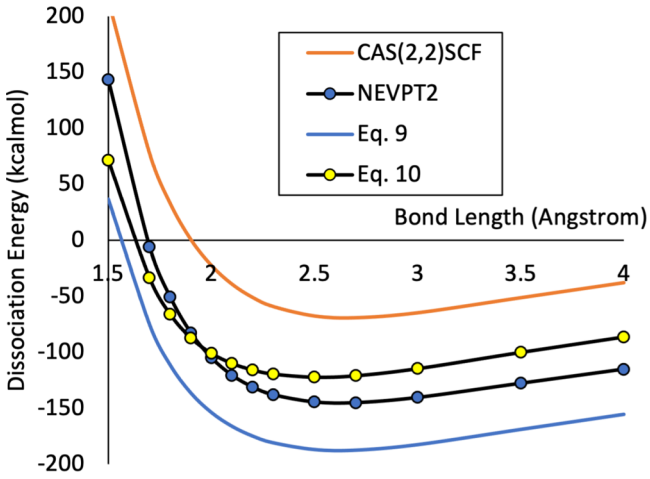

Figure 2. Doubly excited $^1\Sigma_u^+$ potential energy surface of chlorine dimer Cl_2, energy relative to Cl^+ and Cl^-.

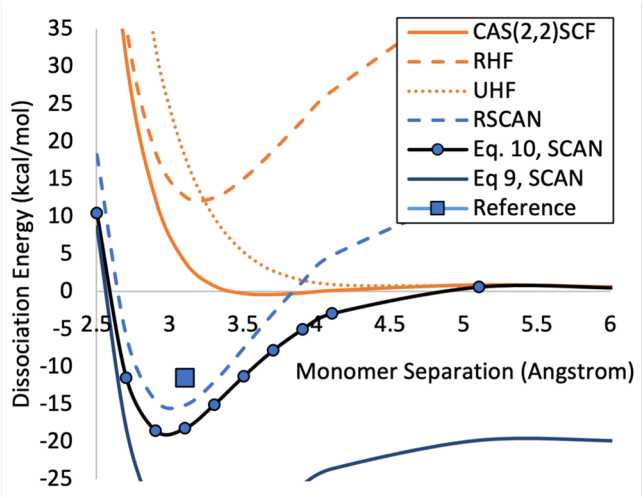

Figure 3. Ground-state singlet potential energy surface of neutral pancake-bonded phenalenyl dimer ply_2, dissociation energies relative to two monomers ply*.

The difference between eq 9 and eq 10 arises from well-known limitations of standard DFAs. Standard DFAs can behave erratically for "abnormal" electron densities where charge or spin delocalizes over multiple centers.[60,61] Such densities occur in strongly correlated systems, including the stretched Cl−Cl bond. The 2e, 2o active space used here ensures that the density abnormality is localized to the active space. Put another way, the densities corresponding to $\hat{\gamma}$ and $\hat{\gamma}^P$ may be abnormal; however the density corresponding to $\hat{\gamma} - \hat{\gamma}^P$ is not. This explains the good performance of eq 10 for dissociation limits. Equation 9 evaluates the density functional on the abnormal densities from $\hat{\gamma}$ and $\hat{\gamma}_P$. Equation 10 only evaluates the density functional on the normal density of the core MOs, $\hat{\gamma} - \hat{\gamma}^P$. Introducing a dependence on the on-top pair density provides another route to modeling the XC energy of abnormal densities.[22]

Multireference calculations are able to effectively treat excited states, including doubly excited states unavailable in the standard adiabatic linear-response formulation of time-dependent DFT. Equation 10 has been applied with standard ground-state DFAs to simulate excited states localized within the active space.[21] Here, we compare eq 9 and eq 10 for the doubly excited $^1\Sigma_u^+$ $(\sigma_g^2 \rightarrow \sigma_u^2)$ state of chlorine dimer. Figure 2 shows the potential energy surface of this excited state, computed relative to the dissociation limit of ground-state Cl^+ and Cl^- ions.[59] The NEVPT2 reference calculations in Figure 2 give a minimum around 5 bohr, bound by 145 kcal/mol relative to Cl^+ and Cl^-. This is somewhat deeper than the 125 kcal/mol well found in ref 59. As for the ground states in Figure 1, eq 10 is close to the NEVPT2 reference, while eq 9 is overbound by ∼40 kcal/mol relative to that reference.

Phenalenyl Dimer. We continue by illustrating eq 9 and eq 10 for the pancake bond of phenalenyl dimer. Figure 3 shows the computed ground-state potential energy surfaces. Calculations use a minimal active space $N_e = N_a = 2$ and compare to CAS(2e,2o)SCF, Hartree−Fock theory, and spin-symmetry-restricted DFT with the SCAN DFA. As seen in previous studies,[33] CAS(2e,2o)SCF severely underbinds at equilibrium, predicting a nearly unbound dimer. Spin-symmetry-restricted Hartree−Fock theory gives a spurious minimum above the energy of two monomers. Breaking spin symmetry removes this spurious minimum and recovers the correct energy at the dissociation limit, but still predicts that the dimer is unbound. Spin-symmetry-restricted DFT gives a reasonable treatment near the minimum, as in previous work,[37] but artificially predicts that the dissociated dimer is above the energy of two monomers, due to incorrect treatment of "strong" correlation at large separations. As discussed in in ref 37, density functional approximations, even approximations that do not include "long-range" dispersion, can provide reasonable predictions for pancake bond energies and bond lengths near equilibrium. More broadly, density functional approximations that do not include "long-range" dispersion interactions can capture some chemically relevant "medium-range" electron correlation effects in organic chemistry.[57,62] As for chlorine dimer, calculations with eq 9 strongly overbind, due to the limitations of the DFA. Calculations with eq 10 provide a reasonable treatment of the entire potential energy surface, without spin contamination.

Figure 4 illustrates how the choice of density functional approximation affects the predictions of eq 10. Both panels compare spin-symmetry-restricted calculations with eq 10, to the corresponding spin-symmetry-restricted DFT calculation. The left panel shows bond energies at the equilibrium 3.1 Å

https://doi.org/10.1021/acs.jpca.2c08616
J. Phys. Chem. A 2023, 127, 3684−3691

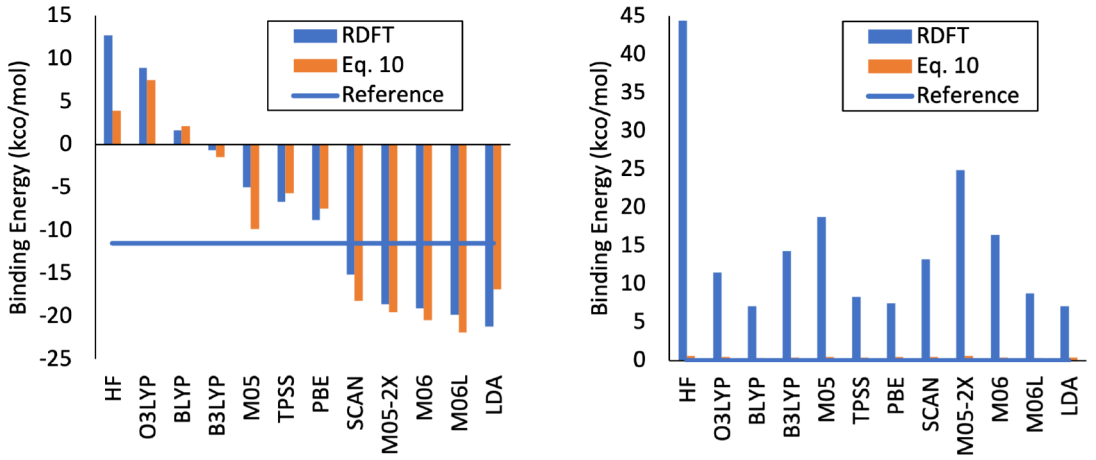

Figure 4. Binding energies of neutral pancake-bonded phenalenyl dimer ply_2, evaluated with eq 10 or spin-restricted DFT, for a variety of density functional approximations. (Left panel) Equilibrium intermonomer separation 3.1 Å. (Right panel) Stretched intermonomer separation 6.1 Å.

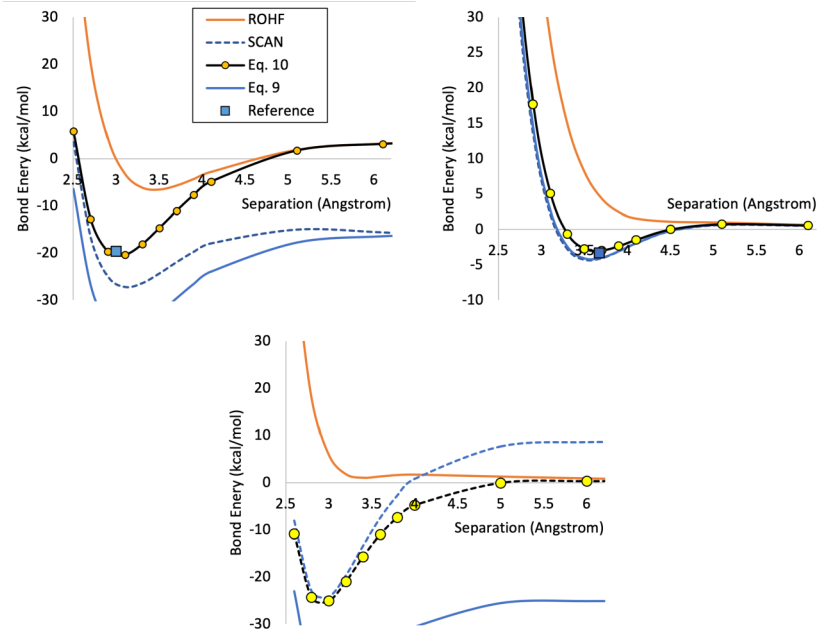

Figure 5. (Left) Ground-state doublet potential energy surface of cationic phenalenyl dimer ply $^{+}_{2}$, dissociation energies relative to ply* and ply^{+}. (Center) Lowest-energy triplet potential energy surface of neutral phenalenyl dimer ply_2, dissociation energy relative to two monomers ply*. (Right) Ground-state singlet potential energy surface of perfluorinated phenalenyl dimer $pfply_2$, dissociation energies relative to two monomers pfply*.

separation reported in ref 33. The right panel shows bond energies computed at a stretched intermonomer separation. Near equilibrium, the bond strength is largely governed by the choice of DFA. Standard DFT and eq 10 give nearly equivalent bond energies, for a variety of different standard approximations. For the stretched separation, the situation is different. Spin-symmetry-restricted DFT behaves erratically, due to the delocalization errors described above. In contrast, eq 10 gives reasonable and negligible bond energies with all of the tested density functional approximations.

Figure 5 illustrates eq 9 and eq 10 for the half-pancake bond[42] of the cationic phenalenyl dimer, the lowest-energy triplet state of the neutral phenalenyl dimer, and the singlet ground state of the perfluorinated phenalenyl dimer.[63] The minimal active space for the cationic dimer includes only one bonding electron, making the CAS(1e,1o)SCF wave function equivalent to restricted open-shell Hartree−Fock. The minimal active space for the neutral triplet dimer includes two same-spin electrons, making the CAS(2e,2o)SCF wave function equivalent to restricted open-shell Hartree−Fock. Equation 9 and SCAN DFT both overbind the cationic dimer and give reasonable results for the triplet dimer. Equation 10 avoids the large delocalization error[64] and overbound dissociation limits of the cationic dimer, while also providing a very accurate treatment of the reference[35] binding energies at equilibrium for both dimers. Trends for the perfluorinated dimer are consistent with the unfluorinated dimer.

Figure 6 shows predicted potential energy surfaces for a doubly excited singlet state of the neutral phenalenyl dimer, analogous to the doubly excited state of Cl_2 in Figure 2. We compute this as the first singlet excited state from a state-averaged CAS(2e,2o)SCF calculation on phenalenyl dimer. As in Figure 2, this state dissociates into charged closed-shell species phe^{+}-phe^{-} ↔ phe^{-}-phe^{+}. As in Figure 2, calculations

https://doi.org/10.1021/acs.jpca.2c08616
J. Phys. Chem. A 2023, 127, 3684−3691

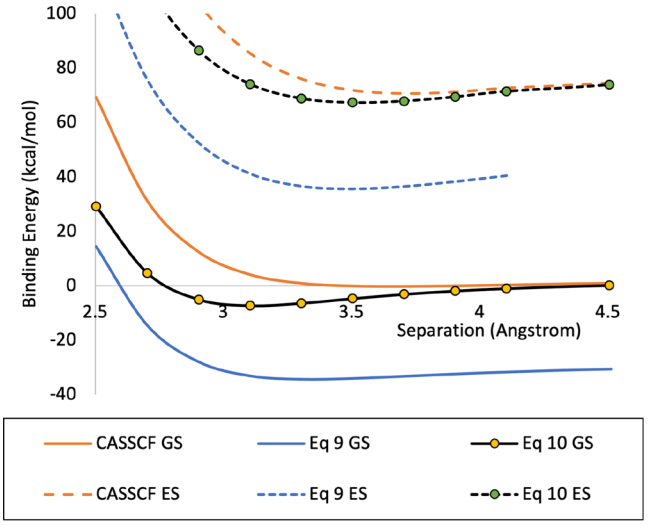

Figure 6. Ground- and excited-state singlet potential energy surfaces of phenalenyl dimer, dissociation energies relative to two ply* molecules.

with eq 10 are close to the CASSCF value, while calculations with eq 9 overstabilize the excited state.

DISCUSSION

The present work demonstrates how the adiabatic projection approach can aid development of wave function-in-DFT approximations capable of modeling large systems. We show that the wavefunction-in-DFT approximation derived in ref 25 (eq 9) can be extended to provide a formal justification for the *ansatz* of ref 21 (eq 10). Systematic comparisons between these two approaches show that eq 10 is more suitable for modeling dissociating bonds, due to its effective treatment of DFT approximations' systematic errors for "abnormal" densities. We also show that eq 10 provides a viable strategy for modeling delocalized pancake bonding, recovering the performance of standard DFT near equilibrium,[37] while also giving a reasonable treatment of the dissociation limit. Overall, the results motivate continued formal investigation of wave-function-in-DFT approaches. Our results also motivate applying the projected interaction correction to other large pancake-bonded systems.[63,65]

AUTHOR INFORMATION

Corresponding Author

Benjamin G. Janesko − *Department of Chemistry & Biochemistry, Texas Christian University, Fort Worth, Texas 75039, United States;* orcid.org/0000-0002-2572-5273; Email: b.janesko@tcu.edu

Author

Luis Rizo − *Intense Laser Physics Theory Unit, Illinois State University, Normal, Illinois 61790, United States*

Complete contact information is available at: https://pubs.acs.org/10.1021/acs.jpca.2c08616

Notes

The authors declare no competing financial interest.

ACKNOWLEDGMENTS

This work was supported by the National Science Foundation Research Experiences for Undergraduates program PHY-1659444. The authors acknowledges the Texas Advanced Computing Center at the University of Texas at Austin for providing HPC resources that have contributed to the research results reported within this paper.

REFERENCES

(1) Kong, J.; Proynov, E.; Yu, J.; Pachter, R. Describing a Strongly Correlated Model System with Density Functional Theory. *J. Phys. Chem. Lett.* **2017**, *8*, 3142−3146.
(2) Becke, A. D. Excited-state surfaces of ethylene from the B13 strong-correlation density functional. *Mol. Phys.* **2015**, *113*, 1884−1889.
(3) Shao, Y.; Head-Gordon, M.; Krylov, A. I. The spin−flip approach within time-dependent density functional theory: Theory and applications to diradicals. *J. Chem. Phys.* **2003**, *118*, 4807−4818.
(4) Roemelt, M.; Krewald, V.; Pantazis, D. A. Exchange Coupling Interactions from the Density Matrix Renormalization Group and N-Electron Valence Perturbation Theory: Application to a Biomimetic Mixed-Valence Manganese Complex. *J. Chem. Theory Comput.* **2018**, *14*, 166−179.
(5) Shu, Y.; Truhlar, D. G. Doubly Excited Character or Static Correlation of the Reference State in the Controversial 2 ^1A_g State of *trans*-Butadiene? *J. Am. Chem. Soc.* **2017**, *139*, 13770−13778.
(6) Langer, M.; Paloncýová, M.; Medved, M.; Pykal, M.; Nachtigallová, D.; Shi, B.; Aquino, A. J.; Lischka, H.; Otyepka, M. Progress and challenges in understanding of photoluminescence properties of carbon dots based on theoretical computations. *Appl. Mater. Today* **2021**, *22*, 100924.
(7) Sharma, P.; Bernales, V.; Knecht, S.; Truhlar, D. G.; Gagliardi, L. Density matrix renormalization group pair-density functional theory (DMRG-PDFT): singlet−triplet gaps in polyacenes and polyacetylenes. *Chemical Science* **2019**, *10*, 1716−1723.
(8) Janesko, B. G. Replacing hybrid density functional theory: motivation and recent advances. *Chem. Soc. Rev.* **2021**, *50*, 8470.
(9) Sayfutyarova, E. R.; Sun, Q.; Chan, G. K.-L.; Knizia, G. Automated Construction of Molecular Active Spaces from Atomic Valence Orbitals. *J. Chem. Theory Comput.* **2017**, *13*, 4063−4078.
(10) Bao, J. J.; Truhlar, D. G. Automatic Active Space Selection for Calculating Electronic Excitation Energies Based on High-Spin Unrestricted Hartree−Fock Orbitals. *J. Chem. Theory Comput.* **2019**, *15*, 5308−5318.
(11) Savin, A. A Combined Density Functional and Configuration Interaction Method. *Int. J. Quantum Chem.* **1988**, *34*, 59−69.
(12) Kraka, E. Homolytic dissociation energies from GVB-LSDC calculations. *Chem. Phys.* **1992**, *161*, 149−153.
(13) Savin, A.; Flad, H.-J. Density functionals for the Yukawa electron-electron interaction. *Int. J. Quantum Chem.* **1995**, *56*, 327−332.
(14) Malcolm, N. O. J.; McDouall, J. J. W. Combining Multi-configurational Wave Functions with Density Functional Estimates of Dynamic Electron Correlation. *J. Phys. Chem.* **1996**, *100*, 10131−10134.
(15) Yang, W. Generalized adiabatic connection in density functional theory. *J. Chem. Phys.* **1998**, *109*, 10107−10110.
(16) Gräfenstein, J.; Cremer, D. The combination of density functional theory with multi-configuration methods − CAS-DFT. *Chem. Phys. Lett.* **2000**, *316*, 569−577.
(17) Toulouse, J.; Colonna, F.; Savin, A. Long-range−short-range separation of the electron-electron interaction in density-functional theory. *Phys. Rev. A* **2004**, *70*, 062505.
(18) Fromager, E.; Toulouse, J.; Jensen, H. J. A. On the universality of the long-/short-range separation in multiconfigurational density-functional theory. *J. Chem. Phys.* **2007**, *126*, 074111.
(19) Toulouse, J.; Gerber, I. C.; Jansen, G.; Savin, A.; Ángyán, J. G. Adiabatic-Connection Fluctuation-Dissipation Density-Functional

Theory Based on Range Separation. *Phys. Rev. Lett.* **2009**, *102*, 096404.
(20) Li Manni, G.; Carlson, R. K.; Luo, S.; Ma, D.; Olsen, J.; Truhlar, D. G.; Gagliardi, L. Multiconfiguration Pair-Density Functional Theory. *J. Chem. Theory Comput.* **2014**, *10*, 3669−3680.
(21) Pijeau, S.; Hohenstein, E. G. Improved Complete Active Space Configuration Interaction Energies with a Simple Correction from Density Functional Theory. *J. Chem. Theory Comput.* **2017**, *13*, 1130−1146.
(22) Pernal, K.; Hapka, M. Range-separated multiconfigurational density functional theory methods. *WIREs Computational Molecular Science* **2022**, *12*, 1.
(23) Sharma, P.; Bao, J. J.; Truhlar, D. G.; Gagliardi, L. Multiconfiguration Pair-Density Functional Theory. *Annu. Rev. Phys. Chem.* **2021**, *72*, 541−564.
(24) Janesko, B. G. Adiabatic projection: Bridging ab initio, density functional, semiempirical, and embedding approximations. *J. Chem. Phys.* **2022**, *156*, 014111.
(25) Janesko, B. G. Systematically Improvable Generalization of Self-Interaction Corrected Density Functional Theory. *J. Phys. Chem. Lett.* **2022**, *13*, 5698−5702.
(26) Hedegaard, E. D.; Knecht, S.; Kielberg, J. S.; Jensen, H. J. A.; Reiher, M. Density matrix renormalization group with efficient dynamical electron correlation through range separation. *J. Chem. Phys.* **2015**, *142*, 224108.
(27) Perdew, J. P.; Zunger, A. Self-interaction correction to density-functional approximations for many-electron systems. *Phys. Rev. B* **1981**, *23*, 5048−5079.
(28) Kertesz, M. Pancake Bonding: An Unusual Pi-Stacking Interaction. *Chem.—Eur. J.* **2019**, *25*, 400−416.
(29) Pal, S. K.; Itkis, M. E.; Tham, F. S.; Reed, R. W.; Oakley, R. T.; Haddon, R. C. Resonating Valence-Bond Ground State in a Phenalenyl-Based Neutral Radical Conductor. *Science* **2005**, *309*, 281−284.
(30) Cui, Z.-h.; Lischka, H.; Mueller, T.; Plasser, F.; Kertesz, M. Study of the Diradicaloid Character in a Prototypical Pancake-Bonded Dimer: The Stacked Tetracyanoethylene (TCNE) Anion Dimer and the Neutral $K^{2+}(TCNE)^{2-}$ Complex. *ChemPhysChem* **2014**, *15*, 165−176.
(31) Morita, Y.; Suzuki, S.; Fukui, K.; Nakazawa, S.; Kitagawa, H.; Kishida, H.; Okamoto, H.; Naito, A.; Sekine, A.; Ohashi, Y.; et al. Thermochromism in an organic crystal based on the coexistence of σ- and π-dimers. *Nat. Mater.* **2008**, *7*, 48−51.
(32) Zhang, Y.; Siskin, M.; Gray, M. R.; Walters, C. C.; Rodgers, R. P. Mechanisms of Asphaltene Aggregation: Puzzles and a New Hypothesis. *Energy Fuels* **2020**, *34*, 9094−9107.
(33) Small, D.; Zaitsev, V.; Jung, Y.; Rosokha, S. V.; Head-Gordon, M.; Kochi, J. K. Intermolecular π-to-π Bonding between Stacked Aromatic Dyads. Experimental and Theoretical Binding Energies and Near-IR Optical Transitions for Phenalenyl Radical/Radical versus Radical/Cation Dimerizations. *J. Am. Chem. Soc.* **2004**, *126*, 13850−13858.
(34) Cui, Z.-h.; Lischka, H.; Beneberu, H. Z.; Kertesz, M. Rotational Barrier in Phenalenyl Neutral Radical Dimer: Separating Pancake and van der Waals Interactions. *J. Am. Chem. Soc.* **2014**, *136*, 5539−5542.
(35) Cui, Z.-h.; Wang, M.-h.; Lischka, H.; Kertesz, M. Unexpected Charge Effects Strengthen π − Stacking Pancake Bonding. *JACS Au* **2021**, *1*, 1647−1655.
(36) Cui, Z.-h.; Gupta, A.; Lischka, H.; Kertesz, M. Concave or convex π-dimers: the role of the pancake bond in substituted phenalenyl radical dimers. *Phys. Chem. Chem. Phys.* **2015**, *17*, 23963−23969.
(37) Mou, Z.; Tian, Y.-H.; Kertesz, M. Validation of density functionals for pancake-bonded π − *pi* dimers: dispersion is not enough. *Phys. Chem. Chem. Phys.* **2017**, *19*, 24761−24768.
(38) Leininger, T.; Stoll, H.; Werner, H.-J.; Savin, A. Combining long-range configuration interaction with short-range density functionals. *Chem. Phys. Lett.* **1997**, *275*, 151−160.
(39) Savin, A. Models and corrections: Range separation for electronic interaction—Lessons from density functional theory. *J. Chem. Phys.* **2020**, *153*, 160901.
(40) Runge, E.; Gross, E. K. U. Density-Functional Theory for Time-Dependent Systems. *Phys. Rev. Lett.* **1984**, *52*, 997−1000.
(41) Gräfenstein, J.; Cremer, D. Development of a CAS-DFT method covering non-dynamical and dynamical electron correlation in a balanced way. *Mol. Phys.* **2005**, *103*, 279−308.
(42) Janesko, B. G.; Brothers, E. N. Half-Pancake Bonding in Asphaltenes. *Energy Fuels* **2021**, *35*, 15657.
(43) Pijeau, S.; Foster, D.; Hohenstein, E. G. Excited-State Dynamics of 2-(2′-Hydroxyphenyl)benzothiazole: Ultrafast Proton Transfer and Internal Conversion. *J. Phys. Chem. A* **2017**, *121*, 4595−4605.
(44) Sun, Q.; Zhang, X.; Banerjee, S.; Bao, P.; Barbry, M.; Blunt, N. S.; Bogdanov, N. A.; Booth, G. H.; Chen, J.; Cui, Z.-H.; et al. Recent developments in the PySCF program package. *J. Chem. Phys.* **2020**, *153*, 024109.
(45) Levine, B. G.; Durden, A. S.; Esch, M. P.; Liang, F.; Shu, Y. CAS without SCF—Why to use CASCI and where to get the orbitals. *J. Chem. Phys.* **2021**, *154*, 090902.
(46) Weigend, F.; Ahlrichs, R. Balanced basis sets of split valence, triple zeta valence and quadruple zeta valence quality for H to Rn: Design and assessment of accuracy. *Phys. Chem. Chem. Phys.* **2005**, *7*, 3297.
(47) LISCHKA, H.; DALLOS, M.; SHEPARD, R. Analytic MRCI gradient for excited states: formalism and application to the n-π valence- and n-(3s,3p) Rydberg states of formaldehyde. *Mol. Phys.* **2002**, *100*, 1647−1658.
(48) Vosko, S. H.; Wilk, L.; Nusair, M. Accurate spin-dependent electron liquid correlation energies for local spin density calculations: a critical analysis. *Can. J. Phys.* **1980**, *58*, 1200−1211.
(49) Becke, A. D. Density-functional exchange-energy approximation with correct asymptotic behavior. *Phys. Rev. A* **1988**, *38*, 3098−3100.
(50) Lee, C.; Yang, W.; Parr, R. G. Development of the Colle-Salvetti correlation-energy formula into a functional of the electron density. *Phys. Rev. B* **1988**, *37*, 785−789.
(51) Tao, J.; Perdew, J. P.; Staroverov, V. N.; Scuseria, G. E. Climbing the Density Functional Ladder: Nonempirical Meta−Generalized Gradient Approximation Designed for Molecules and Solids. *Phys. Rev. Lett.* **2003**, *91*, 146401.
(52) Sun, J.; Ruzsinszky, A.; Perdew, J. P. Strongly Constrained and Appropriately Normed Semilocal Density Functional. *Phys. Rev. Lett.* **2015**, *115*, 036402.
(53) Zhao, Y.; Truhlar, D. G. A New Local Density Functional for Main-group Thermochemistry, Transition Metal Bonding, Thermochemical Kinetics, and Noncovalent Interactions. *J. Chem. Phys.* **2006**, *125*, 194101.
(54) Yu, H. S.; He, X.; Truhlar, D. G. MN15-L: A New Local Exchange-Correlation Functional for Kohn−Sham Density Functional Theory with Broad Accuracy for Atoms, Molecules, and Solids. *J. Chem. Theory Comput.* **2016**, *12*, 1280−1293.
(55) Becke, A. D. Density-functional thermochemistry. III. The role of exact exchange. *J. Chem. Phys.* **1993**, *98*, 5648−5652.
(56) Cohen, A. J.; Handy, N. C. Dynamic correlation. *Mol. Phys.* **2001**, *99*, 607−615.
(57) Zhao, Y.; Truhlar, D. G. A Density Functional That Accounts for Medium-range Correlation Energies in Organic Chemistry. *Org. Lett.* **2006**, *8*, 5753−5755.
(58) Perdew, J. P.; Burke, K.; Ernzerhof, M. Generalized Gradient Approximation Made Simple. *Phys. Rev. Lett.* **1996**, *77*, 3865−3868.
(59) Peyerimhoff, S. D.; Buenker, R. J. Electronically excited and ionized states of the chlorine molecule. *Chem. Phys.* **1981**, *57*, 279−296.
(60) Perdew, J. P.; Ernzerhof, M.; Burke, K.; Savin, A. On-top pair-density interpretation of spin density functional theory, with applications to magnetism. *Int. J. Quantum Chem.* **1997**, *61*, 197−205.

https://doi.org/10.1021/acs.jpca.2c08616
J. Phys. Chem. A 2023, 127, 3684−3691

(61) Cohen, A. J.; Mori-Sánchez, P.; Yang, W. Challenges for Density Functional Theory. *Chem. Rev.* **2012**, *112*, 289−320.
(62) Hohenstein, E. G.; Chill, S. T.; Sherrill, C. D. Assessment of the Performance of the M05-2X and M06-2X Exchange-Correlation Functionals for Noncovalent Interactions in Biomolecules. *J. Chem. Theory Comput.* **2008**, *4*, 1996−2000.
(63) Mou, Z.; Kertesz, M. Pancake Bond Orders of a Series of π-Stacked Triangulene Radicals. *Angew. Chem., Int. Ed.* **2017**, *56*, 10188−10191.
(64) Mori-Sánchez, P.; Cohen, A. J.; Yang, W. Localization and Delocalization Errors in Density Functional Theory and Implications for Band-Gap Prediction. *Phys. Rev. Lett.* **2008**, *100*, 146401.
(65) Cui, Z.-h.; Lischka, H.; Beneberu, H. Z.; Kertesz, M. Double Pancake Bonds: Pushing the Limits of Strong $\pi - \pi$ Stacking Interactions. *J. Am. Chem. Soc.* **2014**, *136*, 12958−12965.

https://doi.org/10.1021/acs.jpca.2c08616
J. Phys. Chem. A 2023, 127, 3684−3691